MASTER THESIS

MASTER EN INGENIERIA, CARACTERIZACIÓN Y PROCESADO DE MATERIALES

Agx(SR) NANOCLUSTERS SUPPORTED ON ZEOLITES AS CATALYSTS FOR ENVIRONMENTAL PROCESSES

Álvaro Peinado Terol

Supervised by:

Dr. Noelia Barrabés

Prof. Juan López

Prof. Antonio Eduardo Palomares

September 2018

ACKNOWLEDGMENTS

First, I want to thank my tutor, Dr. Noelia Barrabes for giving me the opportunity to carry out this project and to work with his group in Vienna.

Also give them thanks to the entire group ClusCAT, Vera Truttman, Stephan Pollitt, Clara Garcia and Jon Ostolaza for all your help in the laboratory and out of it during my stay in Vienna.

Furthermore, thanks to all the people from the ITQ, Prof. Fernando Rey, Prof. Antonio Eduardo Palomares, Joaquín Martínez and Irene Lopez for all your help from Valencia.

Finally, to thank my supervisor in Spain Prof. Juan Lopez for their advice and help.

ABSTRACT

In this Master Thesis, the synthesis and isolation of atomically designed silver clusters have been made. The clusters have been prepared with a controlled number of metallic atoms, in particular Ag clusters with 7,25 and 32 atoms of silver have been synthesized. In addition, bimetallic nanoclusters containing 25 atoms of Ag and Au have been also prepared. The nanoclusters have been characterized by different techniques and some of them have been supported on an inorganic material (ITQ-2 zeolite) in order to test their activity for the oxidation of an air pollutant as it is CO. It has been shown that the supported nanoclusters are active catalyst for this reaction and their activity can be related with the type of nanocluster prepared.

Keywords: silver, catalysis, nanoclusters, zeolite, environmental reaction.

RESUMEN

En este trabajo final de máster, se han realizado la síntesis y el aislamiento de grupos de plata de diseño atómico. Los clusters se han preparado con un número controlado de átomos metálicos, en particular se han sintetizado agrupaciones de Ag con 7,25 y 32 átomos de plata. Además, también se prepararon nanoclusters bimetálicos que contienen 25 átomos de Ag y Au. Los nanoclusters se han caracterizado por diferentes técnicas y algunos de ellos han sido soportados en un material inorgánico (zeolita ITQ-2) para probar su actividad para la oxidación de un contaminante del aire como es el CO. Se ha demostrado que los nanoclusters soportados son catalizadores activos para esta reacción y su actividad puede relacionarse con el tipo de nanocluster preparado.

Palabras clave: plata, catálisis, nanoclusters, zeolita, reacción medioambiental

RESUM

En este treball final de màster, s'han realitzat la síntesi i l'aïllament de grups de plata de disseny atòmic. Els clusters s'han preparat amb un número controlat d'àtoms metàl·lics, en particular s'han sintetitzat agrupacions d'Ag amb 7,25 i 32 àtoms de plata. A més, també es van preparar nanoclusters bimetálicos que contenen 25 àtoms d'Ag i Au. Els nanoclusters s'han caracteritzat per diferents tècniques i alguns d'ells han sigut suportats en un material inorgànic (zeolita ITQ- 2) per a provar la seua activitat per a l'oxidació d'un contaminant de l'aire com és el CO. S'ha demostrat que els nanoclusters suportats són catalitzadors actius per a esta reacció i la seua activitat pot relacionar-se amb el tipus de nanocluster preparat.

Paraules clau: plata, catalisis, nanoclusters, zeolita, reacció mediambiental

CONTENTS

LIST OF FIGURES

LIST OF TABLES

1 INTRODUCTION

Metal nanoclusters are an aggrupation of a small number of atoms, that typically measure less than 2nm. They have recently attracted considerable attention due to their exceptional properties that can be adjusted at atomic scale. In the nanoclusters is possible to develop a structure where the exact number of atoms and composition is stablished. This advantage has opened an extense investigation in a large range of applications like nanoelectronics, optics, biomedicine and catalysis. These structures present chemical properties different of larger aggregations with more atoms as nanoparticles or bulks (Figure 1). In this master thesis different silver nanoclusters will be prepared and they will be supported on a zeolite to study their activity for the CO oxidation reaction.

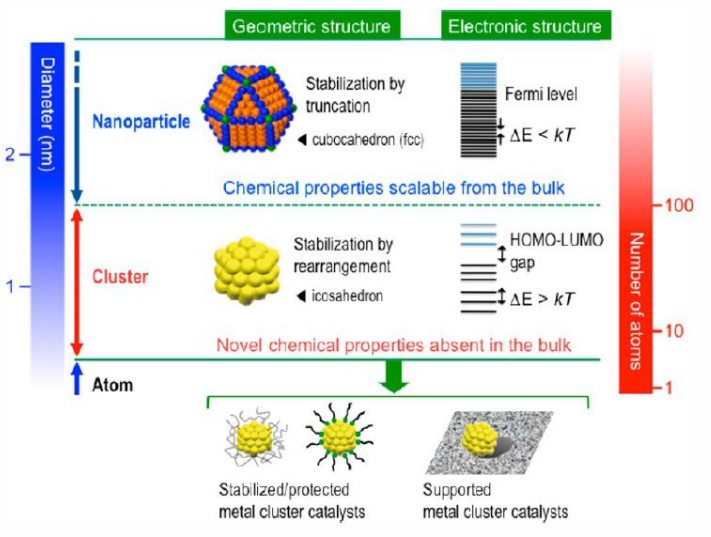

Figure 1: Development of model catalysts based on metal clusters. Graphic reproduced from Yamazoe et al[1]

1.1 NANOCLUSTERS

The nanocluster properties depend on the number of atoms that form it and on how these atoms are structured. For example, the typical structure of a bulk of gold is a face centered cubic (fcc) structure. However, when decreasing the number of atoms in the geometrical structure of gold, different structures can be formed. As can be seen in the Figure 2, the fcc structure of the bulk gold changes when the number of Au atoms decrease from 150 atoms in nanoparticles developing different geometrical structures. In addition, when the number of atoms continue diminishing (clusters), the ratio of surface and core atoms switch completely. This effect produces an excess of energy in the particles that can be used for different applications like catalysis[2].

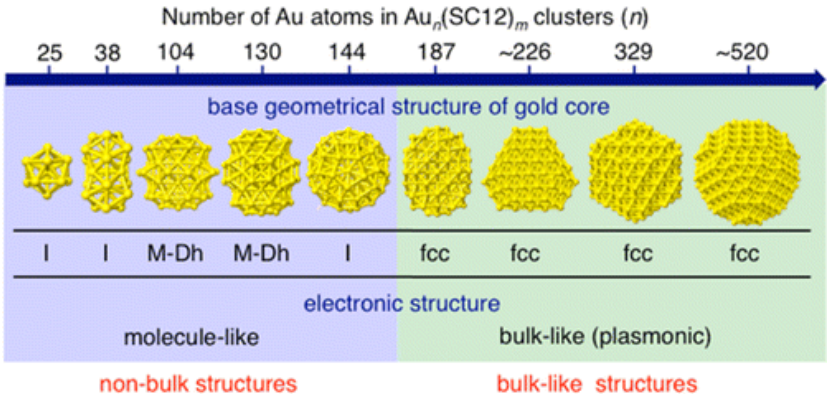

Figure 2: Structures of gold particles from nanoscale to bulk. The graphic was reproduced from *Negishi et al*[3].

Since the discovery of the first sodium clusters by *Brust et al*[4], many different clusters were developed using different metallic atoms. The gold clusters have been the most studied in the last years due to their high stability, their chemical and optical properties and to the possibility of controlling their size with high precision. The most used method to prepare the clusters is the Brush method[4], based on the developing of thiolate protected gold clusters. These clusters have a core of Au atoms surrounded by a cage, formed by alternating Au-S covalent bonds, called staple motif or –S(R)-(Au-S(R)-) oligomer, which stabilize the cluster structure (Figure 3). Each sulphur is bonded to an organic group which is responsible for properties like solubility or chirality, etc[5].

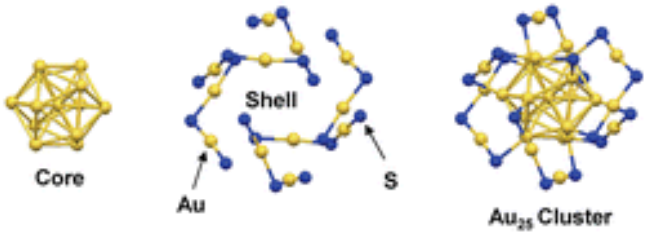

Figure 3: Typical structure of a nanocluster[5].

In this work, silver clusters will be prepared, Ag and Au have different physical and chemical properties despite their similarity in atomic size, structure and bulk-lattice. The differences are more accentuated when going down to nanoscale and even more at nanocluster range where important catalytic properties have been observed.[6] Ag clusters and nanoparticles are potentially useful catalysts in several hydrogenation and oxidation reactions. Recently, Ag nanoclusters supported on mesoporous carbon structures have been described as active catalyst for dehydrogenation reactions with higher activity than another metals such as Pt or Pd[7].

Recently bimetallic nanoclusters have been also described. The doping of this well-known gold nanoclusters with metal atoms like Ag, Hg, Cd, Pd, Pt and Cu enables fine tuning of cluster properties and can increase their stability[10, 11]. This can be explained because changes in atomic composition and coordination leads to different electronic configuration, which then affect the atomic properties. The doping atoms can be located in different positions of the cluster structure, such as the center, core or staples.

Previous works have shown that atomically precise bimetallic clusters have an enhancement effect in several reactions compared to clusters with one metallic specie [12, 13]and this can be related with changes in the electronic configuration depending on the dopant position. Therefore the combination of two metals like silver and gold could be a new method to obtain stable clusters with unique electronic properties[14]

1.2 ZEOLITES

Zeolites are microporous crystalline solids composed of TO4 tetrahedra that extend in all three dimensions, forming a network of cavities and channels that allows its application as catalysts in a host of chemical reactions[15]. Generally, the atom that build the tetrahedron (atom T) is silicon or aluminium, therefore it is said that zeolites are silicates, when the composition is SiO_2, or aluminosilicates when they contain SiO_2 and Al_2O_3. The zeolites structure with cavities and channels, afford to harbor and / or to store molecules or ions that may be required for a specific application[16].

In addition, it must be taken into account that when a silicon atom is replaced in the zeolitic network by an aluminium atom, a negative charge is generated that needs to be compensated by a positive charge in order to guarantee the neutrality of the structure, as well as its stability. For that reason, different cations can be incorporated to the zeolite with important ionic exchange properties.

The generic stoichiometric formula of zeolites is:

$$M_{x/n}\left[(Al_2O_3)_x(SiO_2)_y\right] \times wH_2O$$

The amount of aluminium in the zeolite used to be expressed as the Si / Al ratio. This relationship can take values from one to infinity. This value can never be less than 1 according to Lowenstein's rule, which stipulates that two contiguous aluminium tetrahedrons cannot be together since the electrostatic repulsion between them would be so great that the structure would be destabilized.

Then, it can be stated that zeolites are constructed by assembling a periodic pattern that uses the tetrahedron as a basic building block. Silicon or aluminium are placed in the center of the tetrahedron while the oxygen anions are located in the corners of the tetrahedron, sharing in turn with the adjacent tetrahedron.

Zeolites are a unique type of microporous material with a pore diameter lower than 20Å. The size of the channels depends on the number of tetrahedrons that form them and they can be monodirectional, bidirectional or tridirectional depending on how they are interconnected

in the space directions. This system of channels provides a very high internal surface reaching up to hundreds of square meters per gram of zeolite.

The zeolites can be classified according to their pore size as can be seen in figure 4.

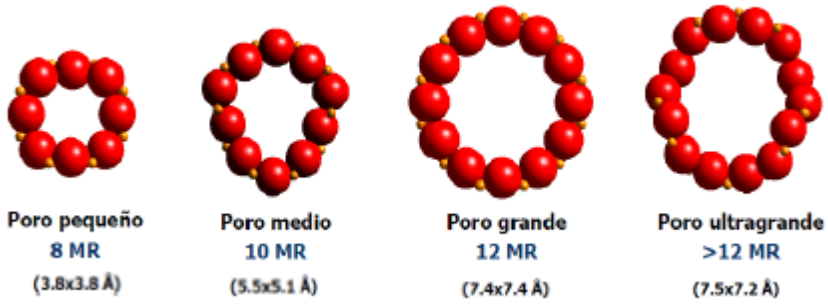

Figure 4 Classification of the zeolites according to the pore size[17].

Thus, there are small, medium, large or ultra large pore zeolites, ranging from 3.5Å to 7.5Å. This classification depends on the number of atoms that make up the pore rings. According to this, the small pores will be formed by rings of 6, 8 or 9 oxygen atoms, the medium ones formed by 10 atoms, the large ones by 12 atoms and the extra-large ones by 14, 18 or 20.

Regarding the catalytic applications of zeolites, the main industrial use is the refining of petroleum in the petrochemical industry although it is also used as a catalyst in many other chemical reactions. Nevertheless, zeolites may have sterical limitations due to the small pores and voids, imposing size constraints on the accessibility to reactants and on the nature of the intermediates and products. Then providing access for larger molecules to the catalytic sites would expand the range of reactions that zeolites can catalyse. In this way, the delamination of the zeolites obtaining layered structure[18] that may improve the accessibility to the catalytic sites. In the figure 5 it is shown the idea of a delaminated zeolite.

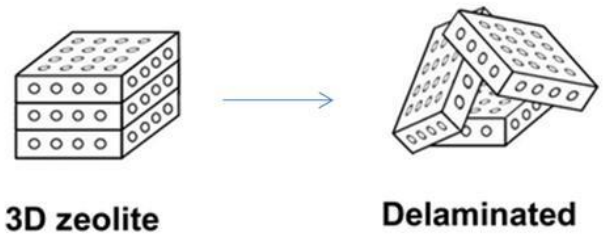

Figure 5: Delaminated zeolite. Graphic reproduced from Opananseko, V., et al[19].

This concept can be very important for adding clusters to delaminated zeolites, as the size of the clusters is too big for being introduced into the pores and voids of the zeolites. So, if a 3D zeolite is impregnated with metallic nanoclusters surely the clusters will be deposited only on the extern surface of the zeolite, covering the channels and reducing the catalytic activity of the zeolite. On the other hand, supporting the clusters on a delaminated zeolite will result in a homogeneous dispersion of the clusters on all the zeolite surface as this zeolite only have external surface. This is idea that is going to be developed in this master thesis, as it is shown in the figure 6.

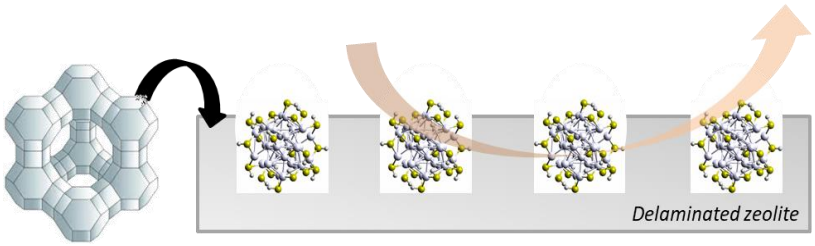

Figure 6: Ag clusters on delaminated zeolite, original figure from Krishnadas*, K. R., et al*[20].

2 AIMS

Many metallic cations [8] especially silver, are used for the enhancement of the catalytic properties of the zeolites [9], but all these studies work with silver nanoparticles and there are not many studies about silver nanoclusters supported on zeolites. The aim of this study is the synthesis and isolation of atomically designed silver clusters and the characterization and study of their physical-chemical properties. The clusters synthesized will be supported on two type of zeolites and their catalytic activity for the CO oxidation will be studied. In particular the next items will be developed in this Master Thesis:

- Synthesis and characterization of stable monometallic thiolated protected silver clusters
- Synthesis and characterization of bimetallic Ag/Au nanoclusters
- Immobilization of the different clusters on different zeolites
- Study the catalytic activity of the zeolites with the clusters for the CO oxidation

It must be pointed out that this Master Thesis was made during my Erasmus stage in the Technical University of Vienna or "Technische Universität Wien", where these clusters have been prepared and characterized. The catalytic experiments have been made in collaboration with the "Instituto de Tecnología Química" from Valencia

3 EXPERIMENTAL PROCEDURE

3.1 CLUSTER SYNHTESIS

Five different silver clusters with different number of silver atoms were synthesized, including a bimetallic Ag-Au cluster. Some of them were supported on two ITQ-2 zeolites with different Si/Al ratio and their activity for the CO oxidation was studied. Table 1 summarize all the clusters synthesized, the ligand used and the dissolvent of the cluster.

Table 1: Summary of the different cluster synthesis

Cluster*	Ag_7	Ag_{32}	Ag_{25}	Ag_{25}	Ag_xAu_{25-x}
Ligand	DMSA	GSH	$HSPhMe_3$	2-PET	$C_{12}H_{25}SH$
Dissolvent	H_2O	H_2O	DCM	Organic solvents	Organic solvents

- **Ag-Clusters with 32 silver atoms**

The synthesis of a cluster of silver with 32 silver atoms ($Ag_{32}SG_{19}$) was made following the bibliography[21] modified with specifications from another published method [22]. According to them, 45 mg of silver nitrate were dissolved in 50 ml of water. Then, 300 mg of glutathione was added into the solution. The solution was cooled in an ice bath for one hour under vigorous stirring. After that an aqueous solution of $NaBH_4$, cooled also in an ice bath, was added dropwise to the mixture. The solution became dark after this addition and it became black after one hour [22]. The mixture was stirring for an hour, and later on was concentrated in a rotary evaporator. The resulting clusters were precipitated and washed with methanol to remove unreacted materials and finally dried and stored at low temperature. The entire reaction was made with a N_2 atmosphere without oxygen in order to avoid the glutathione oxidation. The cluster synthesized was solved on water. All the reagents appear in the table 2.

* The subindex indicate the number of metallic atoms in the cluster

Table 2: Reagents of $Ag_{32}SG_{19}$ synthesis

Reagent	Quantity (mg)
Silver Nitrate ($AgNO_3$)	45
Glutathione (GSH)	300
Sodium Borohydride ($NaBH_4$)	50

- **Ag-Clusters with 7 silver atoms**

Nanoclusters of silver with 7 silver atoms (Ag_7DMSA_4) were synthesized following two reported procedures with some modifications[23, 24]. The reagents used are shown in the table 3. Initially, silver salt was solved in 50 ml of ethanol; this solution was cooled in an ice bath. Then the DMSA was added to the cold solution, this mixture was stirred and kept into the ice bath for 4 hours, the colourless solution turned yellow, showing the presence of the $Ag_x(DMSA)_y$ compound. The $NaBH_4$ was slowly added to the solution under stirring; the yellowish solution turned dark brown, indicating the reduction of the cluster. The sample precipitate spontaneously after 12 hours in the solvent. The sample was centrifugated and the ethanol removed. The cluster was washed and precipitated with methanol to remove the unreactants, then the methanol was removed by centrifugation. This synthesis was made in a N_2 atmosphere to prevent the oxidation of the reactants. The clusters synthesized were solved on water.

Table 3: Reagents of Ag_7DMSA_4 synthesis

Reagent	Quantity (mg)
Silver Nitrate ($AgNO_3$)	46
Dimercapto-succinic Acid (DMSA)	50
Sodium Borohydride ($NaBH_4$)	50

- **Ag-Clusters with 25 silver atoms prepared with trimethylbenzene**

Nanoclusters of silver with 25 atoms (Ag_{25}) cluster synthesized following the Brush method, but using $HSPMe_3$ as ligand instead of $HSPMe_2$, that was the ligand used on the cited article [25]. The procedure for the synthesis was: first, silver salt was solved in 2 mL of methanol with sonication, then $HSPhMe_3$ was added to this solution producing a thick

yellow mixture. After that dichloromethane was added to this mixture and finally a PPh4Br solved in methanol was also added. The quantity of reagents used is shown in Table 4 PPh4Br is a positive counter ion, because the Ag25 clusters are negatively charged and the lack of counter ions during the synthesis produces large nanoparticles instead of clusters. After the addition the colour of the solution changed turning to yellow and then getting dark. After that the solution was stirred for 6 hours and aged overnight at low temperature. The sample was centrifuged obtaining a soft brown supernatant. This supernatant was concentrated in a rotary evaporator and was washed with methanol. The methanol was removed and the clusters were solved again in dichloromethane. This reaction was done under a N_2 atmosphere to avoid the ligand oxidation. The cluster synthesized was solved on dichloromethane.

Table 4: Reagents of $Ag_{25}(HSPhMe_3)$ synthesis

Reagent	Quantity (mg)
Silver Nitrate ($AgNO_3$)	38
Trimethylbenzenethiol ($HSPhMe_3$)	0,09
Sodium Borohydride ($NaBH_4$)	15
Tetraphenylphosphonium Bromide (PPh_4Br)	6

- **Ag-Clusters with 25 silver atoms prepared with 2-PET**

Another procedure was used for the synthesis of Ag nanoclusters with 25 atoms. It is based on a method with modifications to obtain Au_{25} clusters [28]. The procedure consists on: first the silver salt was dissolved in 30 ml of tetrahydrofuran, an organic solvent, then the TOAB was added to the solution forming a yellow coloured solution; under stirring the 2-PET was added to this mixture, before to add the reducing agent ($NaBH_4$) dissolved in water, the solution was kept in an ice bath for two hours. The mixture obtained was evaporated to dryness and cleaned with methanol after one day aged. The quantity of reagents added is shown in table 5. The cluster synthesized was solved in toluene.

Table 5: Reagents of Ag_{25} clusters synthesis

Reagent	Quantity (mg)
Silver Nitrate ($AgNO_3$)	82
2-Phenylethanethiol(2-PET)	345
Sodium Borohydride ($NaBH_4$)	190
Tetraoctylammonium Bromide (TOAB)	410

- **Au-Ag Clusters**

Bimetallic clusters of Ag and Au with 25 atoms ($Au_{25-x}Ag_x$) were also prepared, since several references[26,27]reveal an improvement in the stability and in the catalytic properties of this material comparing with the monometallic clusters. It has been shown that the combination of gold and silver atoms changes the structure of the clusters and this results in an improvement of its properties.

$Au_{25-x}Ag_x$ was synthesized using silver and gold ions as the starting materials. Two solutions were prepared: an aqueous solution of gold and silver precursors, $HAuCl_4$ and $AgNO_3$ respectively and another solution of toluene with tetraoctylammonium bromide (TOAB). The toluene solution was added to the aqueous solution under stirring. After 30 minutes the aqueous phase was removed from the organic phase and the dodecanethiol was added as ligand to the toluene solution. Next an aqueous solution of $NaBH_4$ was added to the mixture as reducing agent. The solution was aged for 3 hours, evaporated to dryness, washed with methanol to remove excess of unreactants and byproducts, solved again in dichloromethane, dried and extracted with acetone. All the reagents used in this synthesis can be seen in the table 6. The clusters synthesized was solved on toluene.

Table 6: Reagents of bimetallic clusters synthesis

Reagent	Quantity (mg)
Chloroauric Acid Tetrahydrate ($HAuCl_4$)	954
Tetraoctylammonium Bromide (TOAB)	211
Dodecanethiol	852
Silver Nitrate ($AgNO_3$)	115
Sodium borohydride ($NaBH_4$)	133

3.2 PURIFICATION OF THE CLUSTERS

The products that were obtained after the synthesis were raw clusters not pure clusters, these raw clusters must be purified and separated into size fractions in order to isolate the different pure clusters with a specific number of metallic atoms that were obtained. For this separation and isolation there are two different methods available, one for clusters soluble in organic solvents known as size exclusion chromatography or SEC and other for water soluble clusters the polyacrylamide gel electrophoresis or PAGE.

Hence the Ag_{32} and Ag_7 dissolved in water were separated using the PAGE method and the $Au_{25-x}Ag_x$ and $Ag_{25}PET$ were dissolved in an organic solvent and separated with the SEC method. The $Ag_{25}HSPhMe_3$ could not be separated because it is a very unstable cluster; instead, it must keep stored at low temperatures and solved in dichloromethane[25].

3.2.1 Size Exclusion Chromatography (SEC)

The SEC is a chromatographic method in which molecules in solution are separated by their size, and in some cases by molecular weight. This method is usually applied to large molecules such as proteins and industrial polymers but it can be used on nanoclusters separation. The chromatography column is packed with fine porous beads which are composed of dextran, agarose or polyacrylamide polymers. The pore sizes of these beads are used to estimate the dimensions of the macromolecules[29].

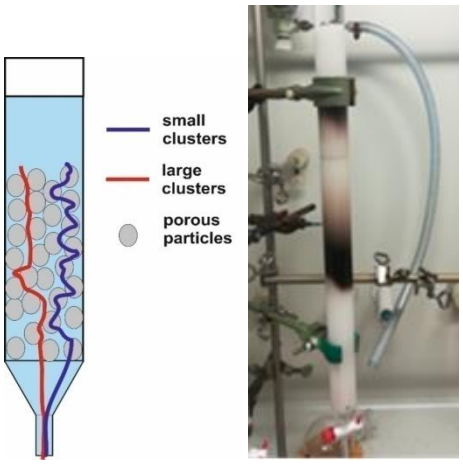

Figure 7: Size Exclusion Chromatography (SEC)

Size exclusion chromatography was performed in a 1000mm×20mm glass column with a frite. The stationary phase was styrene divinylbenzene beads (Bio-Beads S-X1) from Bio-Rad. The clusters were separated using tetrahydrofuran and toluene as solvents. Smaller clusters can enter pores of the stationary phase; therefore, their elution path is longer than for large compounds, leading to shorter retention times for larger clusters. Cluster mixtures were dissolved in minimum amounts of tetrahydrofuran or toluene and applied uniformly on top of the stationary phase. The column was run with about 20drops/min.

This method of separation was performed with the Ag_{25}2-PET and the Ag_xAu_{25-x} clusters, using tetrahydorfurane and toluene as solvents respectively. In both separations four fractions were obtained. These fractions were analyzed after the separation with UV-visible and MALDI-TOF methods to know more about their structure and physicochemical properties, but these results indicate that a better synthesis method is necessary in order to obtain pure fractions.

3.2.2 Polyacrylamide Gel Electrophoresis (PAGE)

The PAGE is a widely used technique to separate molecules depending on their sizes and molecular weight. It is usually applied to separate large molecules as proteins or nucleic acids, but it can be performed for the separation of smaller species as nanoclusters.

An electric field is applied across the gel, causing the different negative charged clusters to migrate across the gel away from the negative electrode and towards the positive electrode; as can be seen in the figure 8. Depending on their size, each cluster moves differently through the gel matrix: small clusters fit through the pores in the gel more easily, while larger ones do it more difficulty. The system is running for a few hours, the time depends on the voltage applied across the gel; separation occurs more quickly at higher voltages, but it is less accurate than with lower voltages. After stablished time, the particles have migrated different distances depending on their size. Nanoclusters with lower number of atoms travel further down the gel, while larger ones stay closer to the initial place[30]. In this case the clusters were separated developing a three-step program: first a voltage of 10 volts was applied for 10 minutes, then in the second step 80 volts were applied for 75 minutes and at last 150 volts were applied for

four hours and a half. With this program it has been shown that is possible the separation of the Ag_7 and the Ag_{32} clusters prepared, as shown in the figure 9 and 10.

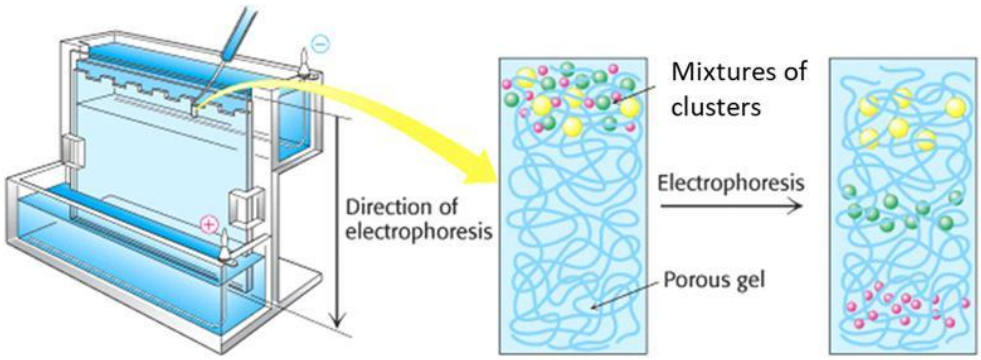

Figure 8: Polyacrylamide Gel Electrophoresis (PAGE). Graphic reproduced from *Basic methods in molecular biology. Elsevier[31]*

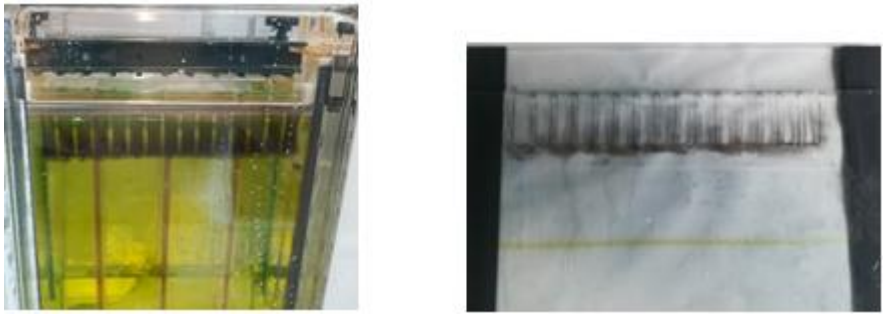

Figure 9: Ag_7DMSA_4 PAGE Separation.

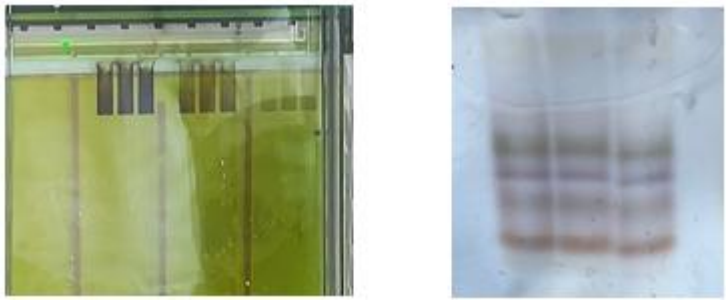

Figure 10: $Ag_{32}SG_{19}$ PAGE Separation.

The figure 9 shows the development of the separation of the Ag_7 through the PAGE, achieving a unique fraction that indicates that the synthesized cluster is pure. In contrast, the

separation of the Ag_{32} shown at figure 10 resulted in six different fractions, indicating that the cluster is not pure, and that the synthesis method used to prepare the cluster was not the appropriate. After the separation process the sample were dissolved again in water and analyzed with UV-visible to know their specific bands and peaks.

3.3 NANOCLUSTERS SUPPORTED ON ZEOLITES

After the synthesis and the separation of the nanoclusters, they were supported on two different ITQ-2 zeolites, they are delaminated zeolites, with different Si/Al ratio. One of them (RTQU46) is a pure silica zeolite and the other (RTQ511) has a relation Si/Al ratio of 10; these zeolites were synthesized and supplied by the "*Instituto de Tecnologia Quimica* (ITQ)" from the Polytechnical University of Valencia.

In order to support the clusters on the zeolites, they were well suspended under ultrasonication, in the same solvent in which the cluster is solved. Then the suspension was stirred and aged during 24 hours, afterwards the sample was dried and stored as it can be seen in the figure 11

Figure 11: Impregnation of the clusters on the zeolite.

With the purpose to test the catalytic properties of the clusters, two different clusters were selected, the $Ag_{25}(HSPhMe_3)$ and the Ag_xAu_{25-x}. They were supported on both zeolites with a weight percentage of 1%; using dichloromethane and toluene as solvents respectively. The prepared catalysts are summarized in table 7.

It must be pointed out that the immobilization of nanoclusters in zeolites is very novel and interesting work as there are few studies reported on nanoclusters supported on alumina materials or silicates, but practically there are not any about the support of these species on zeolites[32-34]

Table 7: Summary table of the clusters impregnated on the zeolites

Sample	Cluster	%wt cluster	Zeolite	Si/Al
Ag_{25}-RTQU46	Ag_{25}	1	RTQU46	∞
Ag_xAu_{25-x}-RTQU46	Ag_xAu_{25-x}	1	RTQU46	∞
Ag_{25}-RTQ511	Ag_{25}	1	RTQ511	10
Ag_xAu_{25-x}-RTQ511	Ag_xAu_{25-x}	1	RTQ511	10

3.4 CHARACTERIZATION TECHNIQUES

The materials prepared have been characterized by different techniques that are described in this point.

- **UV-Visible**

  UV-Vis spectra were recorded on a UV-VIS spectrometer (Perkin Elmer 750 Lambda) in transmission mode. Quartz cuvettes of 10mm path length were used; the solvents used to dissolve the samples were water, tetrahydrofuran, dichloromethane and toluene depending on the sample that was analyzed.

- **Attenuated Total Reflectance (ATR)**

  The ATR spectra were recorded with a Raman microscope system (Renishaw, System 2000; Yobin Yvon, LabRAM HR). The system consists on a light microscope (Leica DL-LM; Olympus BX) coupled to a Raman spectrometer. The excitation laser was an Ar ion laser (k0 = 514 nm, source power 17 mW). Mid- and far-infrared (MIR and FIR) FTIR measurements were performed.

- **Matrix-assisted Laser Desorption/Ionization (MALDI-TOF)**

  Matrix-assisted laser desorption ionization (MALDI) mass spectrometric measurements were performed using a prototype Axima TOF^2 MALDI time-of-flight (TOF)/reflectron (RTOF) mass spectrometer (Shimadzu, Kratos Analytical). For analytical experiments, 2,4,6-trihydroxyacetophenone was selected as MALDI-MS matrix.

- **Electrospray Ionization Mass Spectrometry (ESI)**

The electrospray ionization time-of-flight (ESI-TOF) mass spectras were obtained with a hybrid Maxis Qq-aoTOF mass spectrometer (Bruker Daltonics, Bremen, Germany) fitted with an ESI-source. The samples were injected directly into the chamber at 120 µL·min−1. The instrument parameters were reproduced from Yu et al[35]: capillary voltage, 4 kV; nebulizer, 0.4 bar; dry gas, 2 $L \cdot min^{-1}$ at 120 °C; m/z range, 100−3000.

- **X-Ray Diffraction (XRD)**

For the analysis of the catalyst by X-ray diffraction equipment, the samples are placed in a metallic X-ray sample holder. The sample preparation involves pressing and compaction with the help of a glass sample holder, which guarantees that sample will not be deposited in the diffractometer. The equipment used to carry out the measurements was a PANanlytical CUBIX diffractometer, equipped with an X'Celerator detector using a Cu anode radiation.

- **Thermogravimetry Analysis (TGA)**

The TGA or thermogravimetric analyse the changes of the mass of the samples with the sustained increase of the temperature. The analyses were accomplished in an alumina pan with a Mettler Toledo TGA/SDTA 851e by increasing temperature under flowing air from ambient temperature to 700 ºC at a heating rate of 10 ºC/min.

- **Electronic Microscopy**

Metallic particles sizes were studied on the surface of the zeolite and as crude cluster by electron microscopy in a JEOL-JEM-2100F, microscope operating at 200 kV in transmission (TEM) or scanning transmission electron microscopy (STEM) mode. Before to do the microscopy analysis, the samples were suspended in dichloromethane under ultrasonication for two minutes. Subsequently, the suspension was let to decant and a drop was extracted from the top side and placed on a carbon-coated nickel grid. Metal particle size histograms were generated upon measurement of more than 200 particles from several micrographs taken at different positions on the TEM grid.

3.5 CATALYTIC TESTS

To determine the catalytic activity of the different catalysts, catalytic tests were performed on the reaction equipment described below. The catalysts will be tested for the oxidation reaction of carbon monoxide. The reaction is:

$$CO + \frac{1}{2}O_2 \rightarrow CO_2$$

3.5.1 Reaction System

The reaction system consists of a continuous fixed bed tubular reactor, with control of temperature. The tests were performed at atmospheric pressure.

The equipment used to carry out the reaction is shown in the figure 12:

Figure 12: Equipment for the performance of catalytic tests.

The reaction equipment consists of the following parts:

- Reactor: it is a tubular quartz crystal reactor of 53 cm length and 22 mm of internal diameter. Inside it has a porous quartz plate, where the catalyst is placed during the reaction. It also contains an internal concentric tube in it a K type thermocouple is introduced that allows to measure and control the temperature of the reaction.
- Flow meters: thanks to this device the flow can be regulated and it is possible to control the gases that enter in the reactor. There are as many flow meters, as gases used in the reaction.
- Oven: the oven is a cylindrical metal device, with a hollow inside where the tubular reactor is placed.
- Desiccator: this device is responsible for preventing water from entering the detector. It is a tubular piece of glass with a fixed bed containing $CoCl_2$. It is situated between the reactor outlet and the entrance to the detector.
- Detector: the function of this equipment is to analyze the gaseous flow and to determine the CO concentration. The detector used is a model brand Servomex ServoPro 4900 Series

3.5.2 Catalytic tests

In table 8 are reflected the concentrations of the gas cylinders used in the reaction, the concentration desired in the catalytic tests and the partials flows of the gases for the reaction. The total flow in this reaction is 500 mL/min.

Table 8: Flows and concentrations in the reaction.

Gas	Cylinder concentration (%)	Desired concentration (%)	Flow(mL/min)
CO	4	0,5	63
O_2	21	4	95
N_2	pure	95,5	342
Total	-	-	500

All the catalytic tests are performed with these flows, in order to obtain a total flow of 500 mL/min with 0,5% of CO and 4% of O_2 (N_2 as carrier gas). The mass of catalyst used is approximately 0.25 grams in each catalytic test.

Once set the reaction conditions the following steps were done to perform the experiment:

- Preparation of the catalyst: prior to the start of the catalytic test, the catalyst was prepared to have a grain size between 0.2 and 0.4 mm to prevent preferential and minimize the pressure drop. To get the granulation of the catalyst tablets were prepared in a pressure die, then they were grinded in a mortar and sifted using a sieve to obtain particles of 0.2 to 0.4 mm. After sieving, the catalyst was inserted into the reactor.
- Catalyst activation: activation of the catalyst is made with a O_2 and/or H_2 flow was left to pass one hour at a temperature of 150° C.
- Calibration of the detector: the detector, was calibrated by flowing a stream with a known concentration of CO, the reading of the detector was calibrated to the analytic value known and provided by the CO cylinder specifications.
- Catalytic test: the reaction starts by measuring the CO concentration in the feeding gases, bypassing the reaction system. Once measured the initial concentration, the bypass is closed and the flow is directed to the reactor. The studied temperature range varies from 100°C to 700°C, starting reaction to the maximum temperature. The CO concentration was measured at the exit of the reactor at each temperature (modified in steps of 50°C) until all the temperature range was measured.
- Cleaning equipment: all flow rates were finally set to zero except the nitrogen, which was used to clean the entire system. When the CO analyzer shows a zero concentration of CO, the N_2 flows was also closed and all system reaction was turned off.

4. RESULTS AND DISCUSSION

The main work of this Master Thesis was to prepare the Ag-clusters that were evaluated for the catalytic CO oxidation. Then this chapter will be divided in two main parts, the first one showing the characterization of the material prepared and the second one showing the catalytic activity of selected samples.

4.1 CLUSTER SYNTHESIS

The samples synthesized and separated by SEC and PAGE, were characterized by different methods to stablish their purity and physical chemical properties. Afterwards, the zeolites supported with different clusters were also analyzed by different techniques

4.1.1 UV-Visible

Due to their molecule-like electronic structure, metal nanoclusters exhibit one or more absorption peaks in UV/Vis, that are not observed on agglomeration of metallic atoms as nanoparticles.

The UV spectrum of a nanocluster of Ag with 7 atoms is shown in the figure 13 and compared with the results described on bibliography [24].

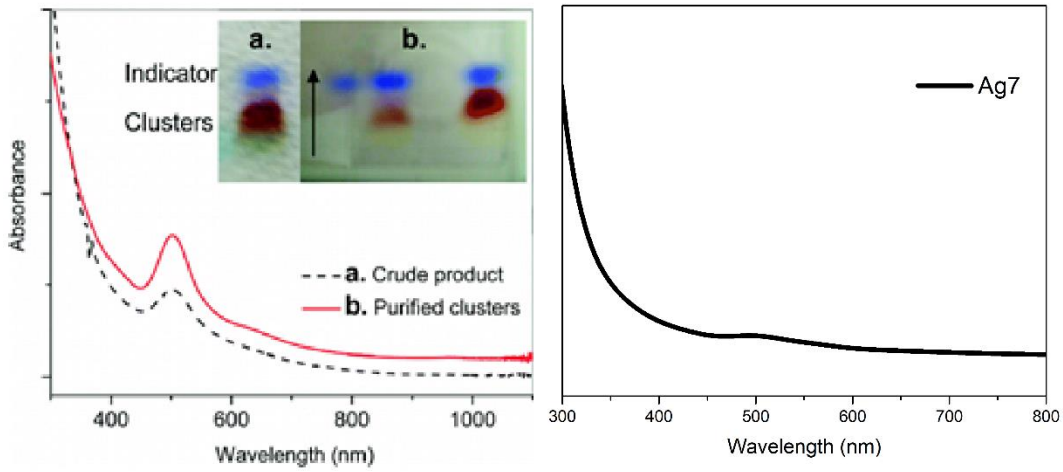

Figure 13: At left the UV-vis spectra of (Ag_7DMSA_4) described in [24]. At right the UV-vis spectra corresponding to the synthesis done in this work.

As it can be seen the UV-Vis absorption spectra of the synthesized Ag_7 clusters dissolved in water shows a weak specific absorption band is it at 500 nanometers. The comparison of this band, with the band assigned to these clusters in bibliography[23, 24](see figure 13 at left) confirms the presence of the same species, suggesting that the synthesis was successful.

In figure 14 is shown the UV-vis spectra corresponding to the $Ag_{25}(HSPhMe_3)$ dissolved in dichloromethane. It has a peak around 400-450 nanometers associated to the Ag nanoclusters. The articles studied [25, 36] also show a specific peak around 450 for these nanoclusters with higher number of Ag atoms, but in the cited papers appear other characteristic peak at 700 nm

for this clusters. These peak it is not observed in the synthesized sample probably due to the ligand used in the synthesis, that in our case was trimethylbenzenethiol instead of the dimethylbenzenethiol used in the reported methods. The reason for this change was the high toxicity of the dimethylbenzenthiol, because of this, it was decided to use the trimethylbenzenethiol, that it is a very similar ligand but much less toxic. Anyway, the peak at 450 nm corresponding to the Ag25, suggest that the cluster has been correctly synthesized.

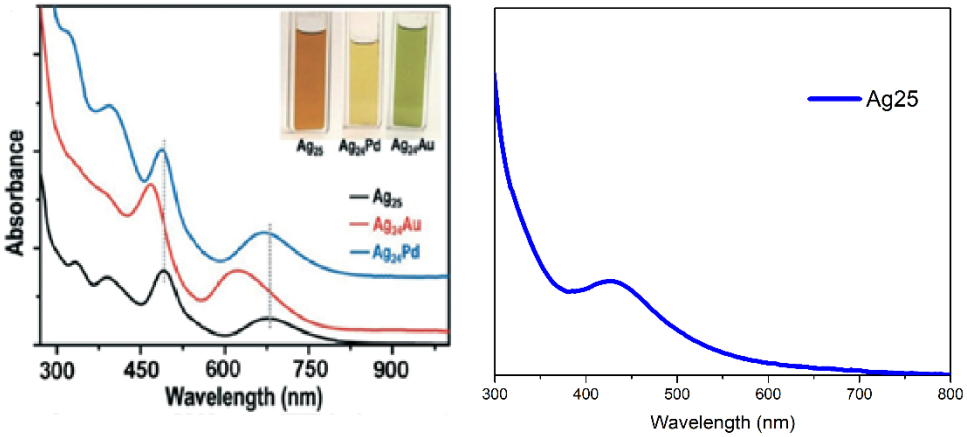

Figure 14: At left the UV-vis spectra of $Ag_{25}(HSPhMe_3)$ described in [25]. At right the UV-vis spectra corresponding to the synthesis done in this work.

The figure 15 shows the UV-vis spectra recorded corresponding to the Ag_{25} with 2-PET as ligand, dissolved in tetrahydrofuran, two and four hours after the synthesis.

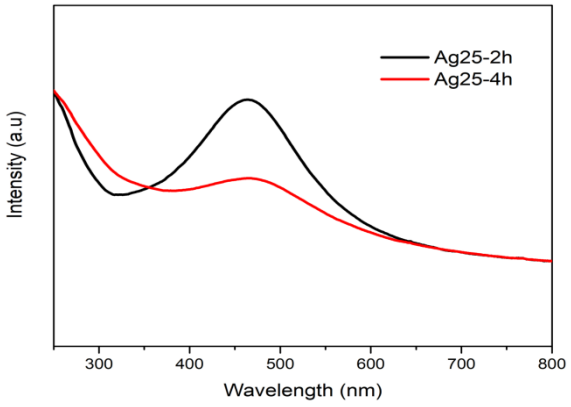

Figure 15: UV-vis spectra of Ag_{25} after two and four hours of the synthesis with 2-PET as ligand.

As it can be see both spectra present a peak around 450 nm related with Ag nanoclusters, this peak is smaller and less pronounced in the sample measured after two hours, while the sample measured after four hours presents a much more pronounced and large peak. This

change suggests that the nanocluster evolute with time, probably join the nanoclusters and creating larger aggregates as nanoparticles.

The UV-vis spectra corresponding to the Ag_{32} cluster is shown at the figure 16. In this graphic it can be seen a very large bond between 400 and 550 nanometers, this band is too broad for a nanocluster, and it does not appear in the articles studied for this synthesis[21, 22]. Therefore, this spectrum can represent particles larger than clusters or a mixture of clusters with different size, as the separation of this sample through the PAGE, have shown (see point 3.2.2) obtaining six different clusters.

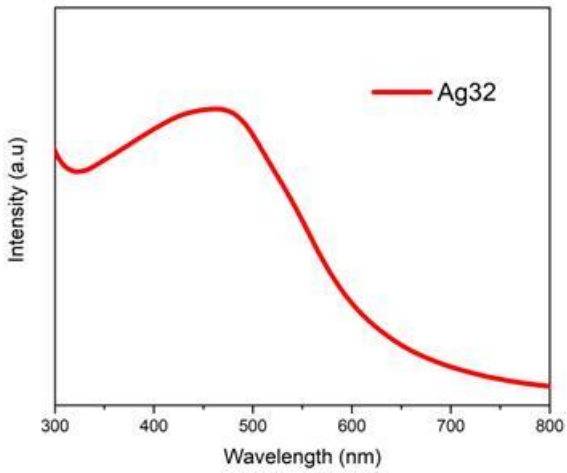

Figure 16: UV-vis spectra of Ag_{32} cluster.

Similar results were expected for the bimetallic nanoclusters because a mixture of phases was obtained in the synthesis as in the separation process.

In the figure 17 and 18 it can be seen the spectra of the different Ag_xAu_{25-x} fractions obtained with SEC and the different Ag_{32} fractions obtained with PAGE respectively.

In the figure 17 is shown the comparison between the Ag_xAu_{25-x} fractions obtained with SEC (right) and bimetallic gold-silver clusters with a different charge of silver from bibliography[26]. The four fractions that were obtained similar bands at 2,8 eV to those described in bibliography[26] as characteristic of Ag-Au nanoclusters with different Au/Ag ratio.

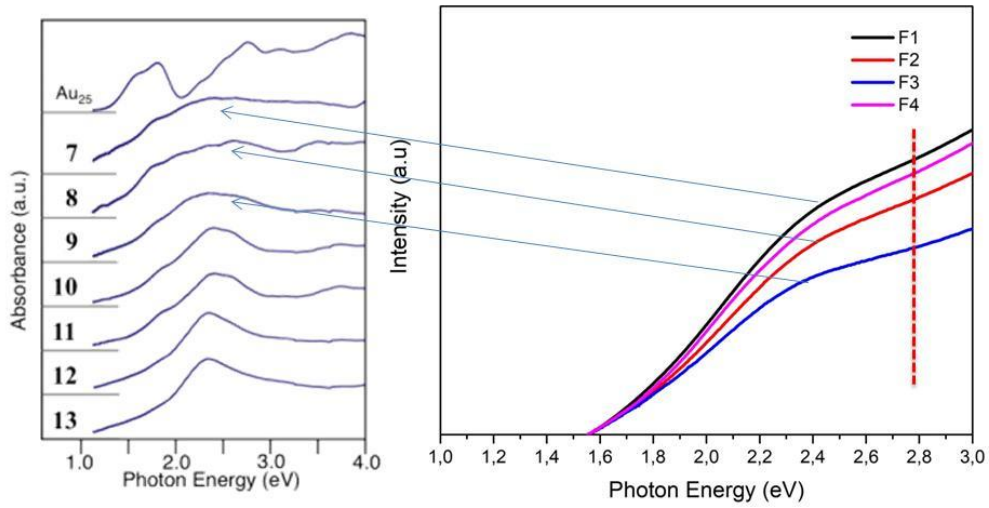

Figure 17: Comparison of different silver-gold clusters UV-vis spectra from a cited article[26] with the fractions obtained after the Ag_xAu_{25-x} separation with SEC.

The figure 18 shows the Ag_{32} fractions separated by PAGE, 6 fractions were obtained and they were analyzed by UV-visible. Each fraction spectra has specifics bands confirming the existence of different type of clusters. Then that synthesis is not very satisfactory because it gets different clusters with a very low yield. On the other hand, the separation confirms the presence of clusters and not nanoparticles, which is a satisfactory result and maybe is possible to improve this process to achieve a synthesis a single cluster.

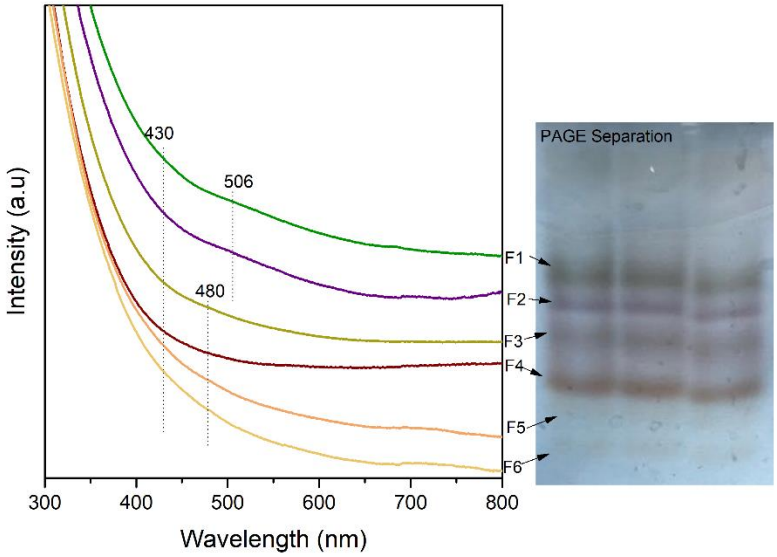

Figure 18: UV-vis spectra of Ag_{32} fractions obtained after the PAGE in nm.

The clusters supported on zeolites were also characterized by UV-vis spectroscopy and the graphics on the figures 19 and 20 compare the UV-visible spectra of the raw zeolites with the spectras of the zeolites containing $Ag_{25}(HSPhMe_3)$ and Ag_XAu_{25-x}.

As it can be seen in figure 19, the spectra corresponding to the pure silica zeolite impregnated with the bimetallic nanocluster (AuAgRTQU46) shows a broad band between 400-600nm, these bands do not appear in the raw zeolite spectra (RTQU46) and maybe indicate the presence of the Ag_XAu_{25-x} nanoclusters into the zeolite. On the other hand, in the spectra corresponding to the zeolite impregnated with silver nanoclusters of 25 atoms (AgRTQU46), not any clear band that points the presence of metallic species in the sample were observed, although it must be taken into account that the use of this technique for solid samples is not so accurate as it was for liquid samples (spectra shown before)

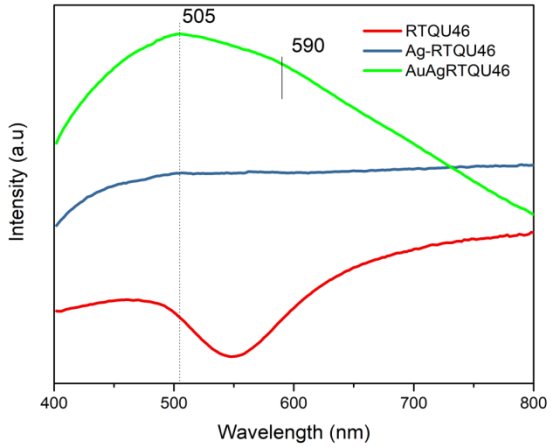

Figure 19: Comparison of UV-vis spectra of the zeolite RTQU46 impregnated with silver clusters, bimetallic clusters and raw zeolite.

The figure 20 shows the UV spectra of the zeolite containing alumina. In this case the sample with silver nanoclusters shows a weak band at 460 nanometers while the bimetallic nanocluster shows another weak band at 527 nanometers. These bands in the doped zeolites maybe point to the presence of metallic species into the zeolites. Nevertheless, as stated before the information obtained with this technique for the solid samples must be carefully considered.

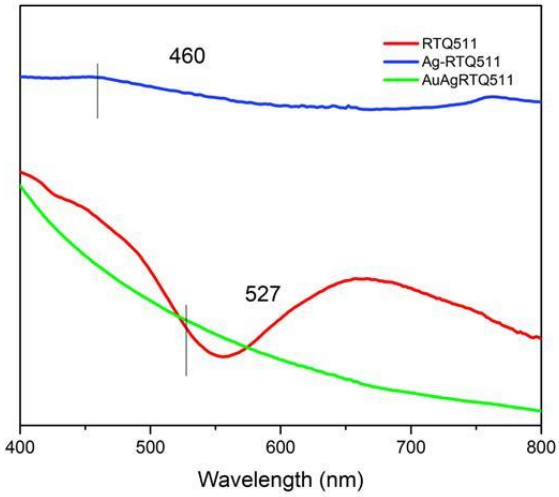

Figure 20: Comparison of UV-vis spectra of the zeolite RTQ511 impregnated with silver clusters, bimetallic clusters and raw zeolite.

4.1.2 Attenuated Total Reflectance (ATR)

Vibrational Spectroscopy is a useful method for studying molecular conformation and properties of nanomaterials. The two raw clusters impregnated in the zeolites, $Ag_{25}(HSPhMe_3)$ and Ag_xAu_{25-x} were measured with this method. The $Ag_{25}(HSPhMe_3)$ far infrared spectra is shown in purple at the figure 21 and the Ag_xAu_{25-x} in yellow at the figure 22. The figure 21 also shows the far infrared spectra of the two zeolites impregnated with the $Ag_{25}(HSPhMe_3)$, the Ag_{25}RTQ511 in blue and the Ag_{25}RTQU46 in green, the two raw zeolites RTQ511 and RTQU46, are represented too with line dotes. The Ag_{25} spectra shows the characteristic peaks related to the bonded thiolate ligands Ag-S, at 220 cm^{-1}, 278 cm^{-1} and 460 cm^{-1}. The Ag_{25}RTQ511 and Ag_{25}RTQU46 spectra do not show the bonded thiolate since the zeolite absorbs all the infrared energy and only it is possible to see the vibrations of the zeolite. In fact, the raw zeolites spectra, in dotted line, show the same bands that the samples doped with the clusters.

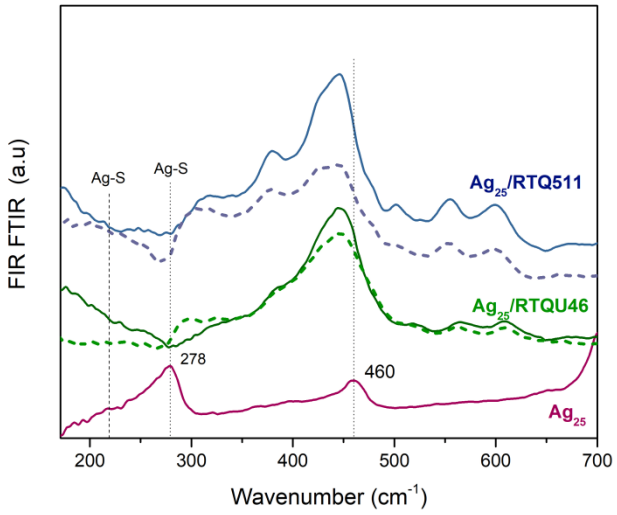

Figure 21: Far infrared spectra of $Ag_{25}(HSPhMe_3)$ nanocluster and zeolites doped with this cluster, in doted lines the spectra of the raw zeolite.

The figure 22 shows the far infrared spectra as in Figure 21, for the bimetallic cluster. The graph shows the cluster in yellow Ag_xAu_{25-x}, and the two zeolites impregnated Ag_xAu_{25-x}RTQ511 and Ag_xAu_{25-x}RTQU46 in blue and green respectively. In this case the Ag_xAu_{25-x} spectra shows an intense peak at 389 cm^{-1} related with the Au-S bond vibrations[37-39], As in the previous case, this peak does not appear in the spectra corresponding to the doped zeolites Ag_xAu_{25-x}RTQ511 and Ag_xAu_{25-x}RTQU46 because zeolite absorbs the infrared energy and only the bands related with the zeolite are observed.

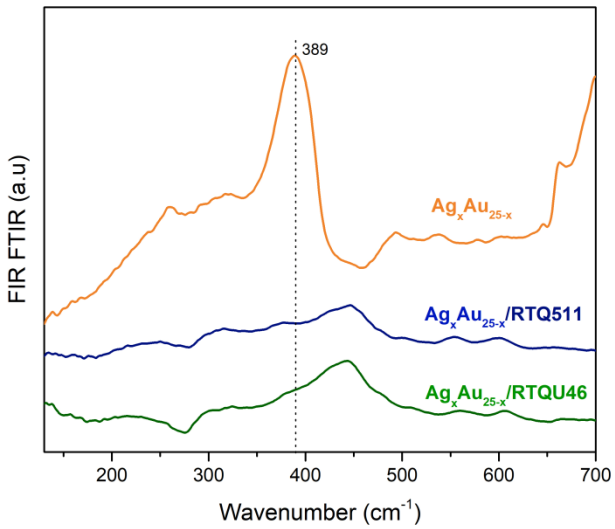

Figure 22: Far infrared spectra of Ag_xAu_{25-x} nanocluster and zeolites doped with this cluster

The figure 23 shows the medium infrared spectra of the two raw clusters impregnated, both spectra shows the absence of peaks around 2500 cm^{-1}, related with the S-H bond vibrations. The lack of this peaks points out that there are no S-H links, which indicates that clusters are stable and do not degrade. Some peaks are observed around 3000 cm^{-1} corresponding with the C-H stretching of the ligands, together with bands at 1250 cm^{-1} characteristic for the deformation of the C-H bonds. The peak at 750 cm^{-1}, corresponds with the C-S bond stretching.

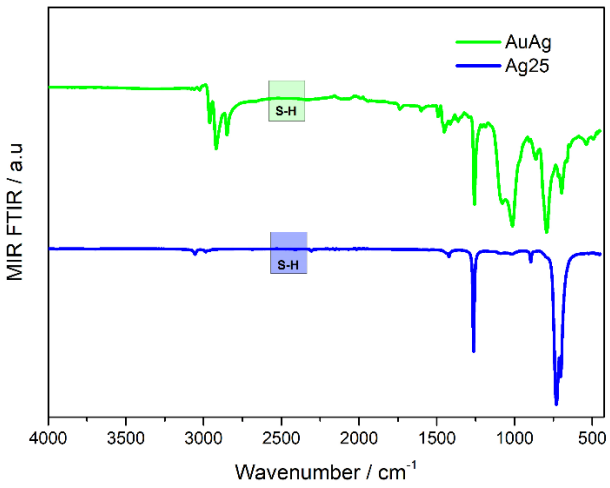

Figure 23: Medium infrared spectra of $Ag_{25}(HSPhMe_3)$ and Ag_xAu_{25-x} nanoclusters

In the figure 24 can be seen the medium infrared spectra of the $Ag_{25}(HSPhMe_3)$, and that of the two zeolites impregnated with the silver cluster Ag_{25}RTQ511 in blue and Ag_{25}RTQU46 in green and the raw zeolites RTQ511 and RTQU46 with dotted lines. As in the far infrared spectra, the zeolite absorbs all the infrared energy, so it is not possible to distinguish the stretching bonds corresponding to the cluster. As before the spectra corresponding to the impregnated zeolites has the same peaks that the spectra of the raw zeolites.

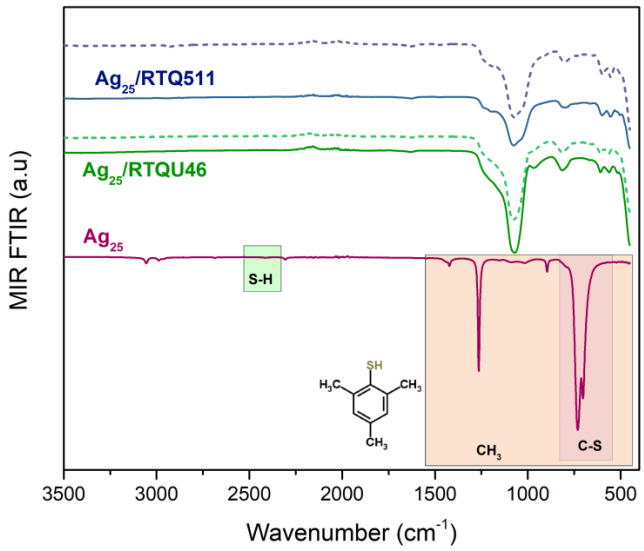

Figure 24: Medium infrared spectra of $Ag_{25}(HSPhMe_3)$ nanocluster and zeolites doped with this cluster, in doted lines the spectra of the raw zeolite.

The figure 25 shows the medium infrared spectra of the Ag_xAu_{25-x}, and that of the two zeolites impregnated with the bimetallic cluster, Ag_xAu_{25-x}RTQ511 in blue and Ag_xAu_{25-x}RTQU46 in green and the raw zeolites RTQ511 and RTQU46 with dotted lines. As in the far infrared spectra, the zeolite absorbs all the infrared energy, so it is not possible to distinguish the stretching bonds corresponding to the cluster. As before the spectra corresponding to the impregnated zeolites has the same peaks that the spectra of the raw zeolites.

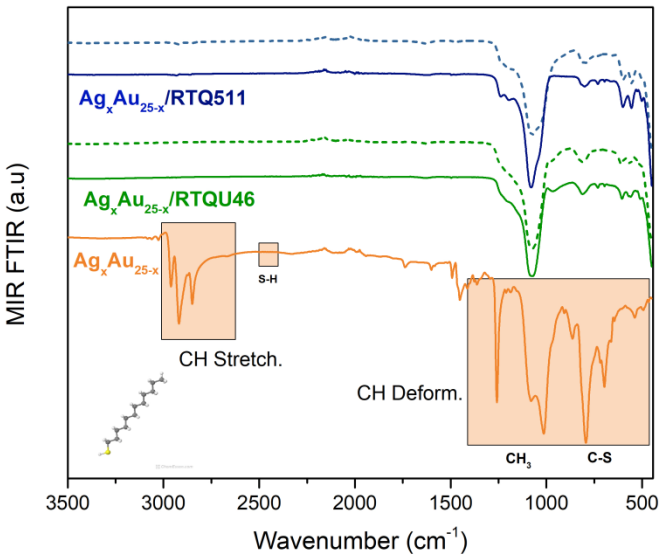

Figure 25: Medium infrared spectra of Ag_xAu_{25-x} nanocluster and zeolites doped with this cluster

4.1.3 Matrix-assisted Laser Desorption/Ionization (MALDI)

For studies of thiolated metal clusters, MALDI is the most frequently applied technique. This technique is very useful because it allows to know the exact formula of the nanocluster studied, analyzing the mass of it

Different sample were studied with this technique in order to know their atomic composition. Three different sample were measured, two fractions from the Ag_{25}2-PET SEC separation, specifically the fraction 2 and 4, and a fraction from the Ag_xAu_{25-x} SEC separation, specifically, the fraction 4. All the measurements were made following reported methods for silver and gold nanocluster MALDI analysis[20, 40].

The figure 26 shows the three spectra recorded with MALDI, however as it can be seen the samples are very fragmented and it is difficult to see the specific peaks clearly. It was not possible to affirm in any of the three cases that the peaks present in the spectra corresponded to the total mass of one of the synthesized clusters. Because of this it was decided to measure these samples using another technique of mass analysis, the electrospray ionization Mass Spectrometry or ESI.

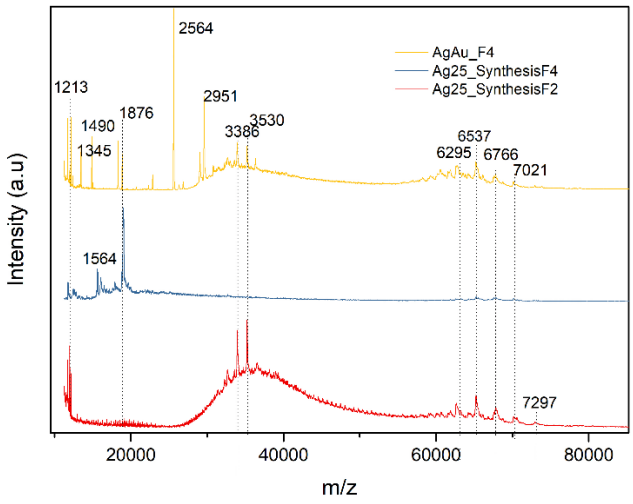

Figure 26: MALDI Spectra of Ag_{25} fractions and Ag_xAu_{25-x} fraction

4.1.4 Electrospray Ionization Mass Spectrometry (ESI-MS)

Electrospray ionization mass spectrometry is a powerful technique similar to MALDI to determine the nanoclusters formula by analyzing the intact nanocluster mass. The same samples analyzed with MALDI were analyzed with ESI, this is the fractions of the Ag_{25}2-PET and the fraction from the Ag_xAu_{25-x}.

Figures 27 and 28 show the spectra of the fraction 2 and 4 from the Ag_{25}2-PET respectively, the range of masses were between 1000 m/z to 2000 m/z, these spectra show different peaks with high intensity that can correspond to silver nanoclusters. However, it was not possible to confirm the presence of any particular species when comparing with the bibliography studied[41, 42].

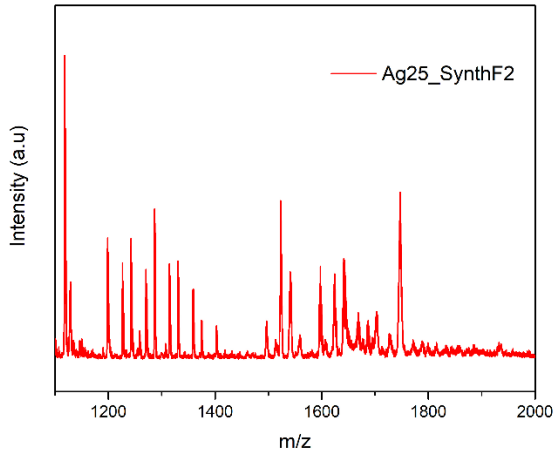

Figure 27: ESI Spectra of the fraction two of Ag_{25}2-PET

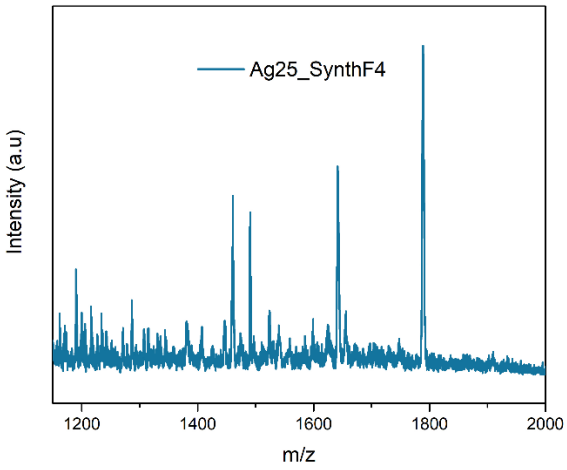

Figure 28: ESI Spectra of the fraction four of Ag_{25}2-PET

The figure 29 shows the fraction four from Ag_xAu_{25-x}, in this case the possible range of analysis was only from 2000 m/z to 2100m/z, in the rest of the range it was not possible to record anything. It can be seen an intense peak at 2060 m/s that could correspond with some bimetallic nanocluster, but it was not possible to check which one in particular[40].

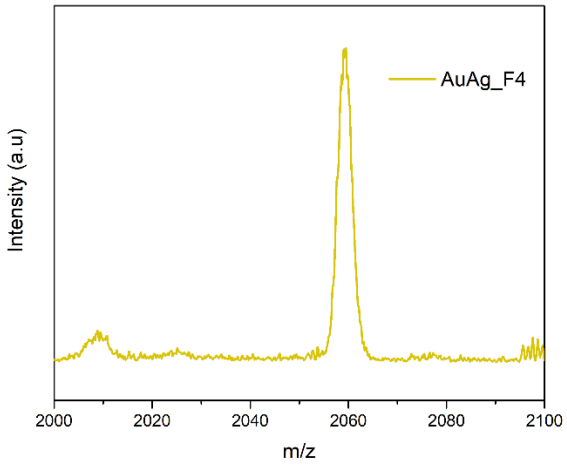

Figure 29: ESI Spectra of the fraction four of Ag_xAu_{25-x}

4.1.5 X-Ray Diffraction

In Figure 30, the diffractograms of the two zeolites RTQU46 and RTQ511 exchanged with the different clusters $Ag_{25}(HSPhMe_3)$ and Ag_XAu_{25-X} are compared in order to analyze if the incorporation of the clusters to the zeolites cause an alteration in the structure of the zeolite

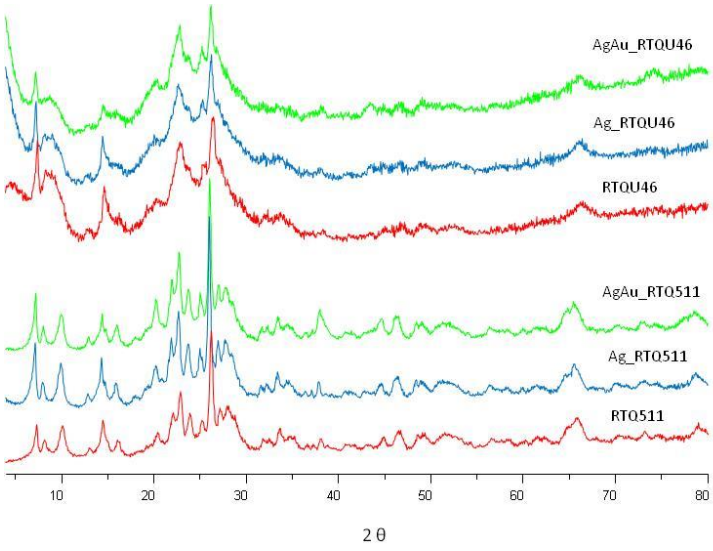

Figure 30: X-Ray Diffraction of the zeolites impregnated with the nanoclusters.

As shown in this figure 30 the position of the diffraction peaks does not vary, and there are no new peaks, which indicates that the crystalline structure of all the samples is not seen modified by introducing the different clusters.

4.1.6 Thermogravimetry Analysis (TGA)

In order to have complementary information about the clusters supported on the zeolites: (Ag_{25}RTQ511, Ag_{25}RTQU46, Ag_xAu_{25-x}RTQ511 and Ag_xAu_{25-x}RTQU46) thermogravimetric analysis was performed. The TGA analysis of the four samples represented in figure 31. As it can be seen Ag_{25}RTQU46 and Ag_xAu_{25-x}RTQU46 show a small weight loss between 150°C and 200°C that is related with the complete removal of the thiolate ligands. Ag_{25}RTQU46 also shows a weight loss at 600°C probably related to the solvent that remains in the sample after the impregnation. AgRTQ511 and Ag_xAu_{25-x}RTQ511 exhibit higher weight loss. AgRTQ511 shows a weight loss at 176°C related with the removal of the ligands but also with the presence of solvent in the sample, as the loss is too big to be only caused by the removal of the ligands. This sample presents another weight loss at 660°C which must also be produced by removing the solvent. Ag_xAu_{25-x}RTQ511 results are similar to AgRTQ511 a first weight loss at 290°C related with the ligands and the solvent, and another loss at 650°C related with the solvents. These analyses confirm the presence of the ligands on the zeolites and therefore the presence and the stability of the clusters on the zeolite.

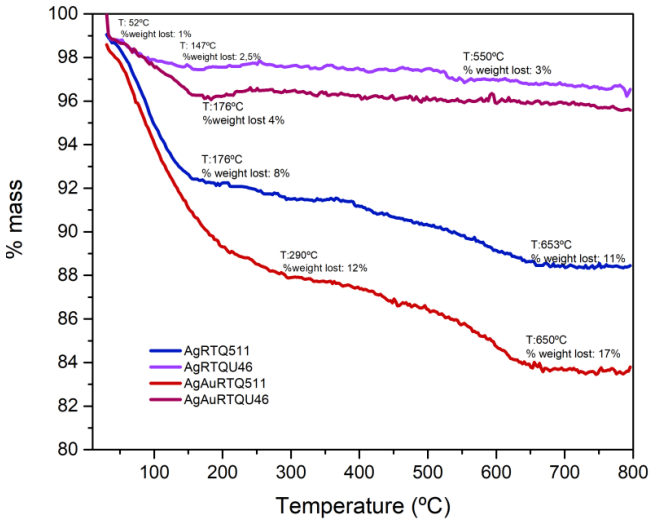

Figure 31: Thermogravimetry Analysis of the zeolites impregnated with nanoclusters.

4.1.8 Electronic Microscopy

The figure 32 shows a high resolution TEM image of the bimetallic nanocluster unsupported, Ag_xAu_{25-x}, a mapping was done in this sample in order to know the different atoms presents in the sample and which metallic atoms are shown in this cluster. The other cluster supported on the zeolites $Ag_{25}HSPhMe_3$ was only analysed once supported on the zeolite, because the raw cluster is not stable in solid state, so it was not possible to analyse this cluster unsupported.

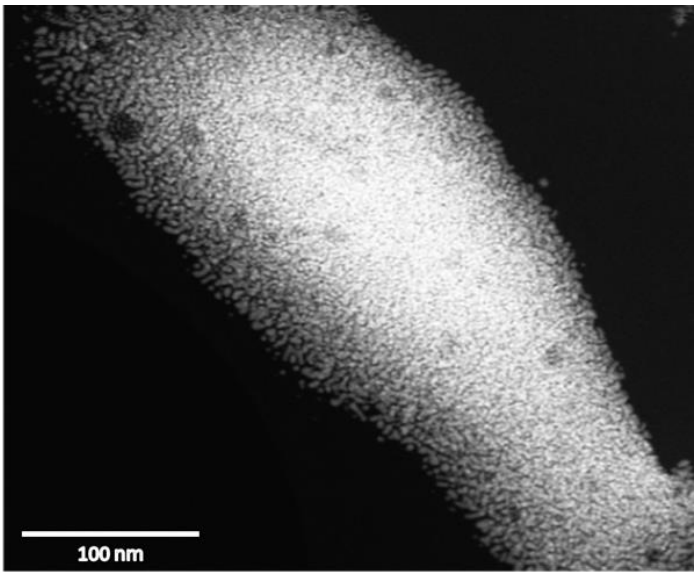

Figure 32: Ag_xAu_{25-x} nanocluster HR-TEM image

In the figure 33 it can be seen the mapping of the TEM image, displaying the signal maps of carbon, gold and silver, using this method, single particles or aggregates with Au and Ag were detected on the unsupported clusters. The mapping of the aggregates shows that the main, metallic component observed in the area analyzed of the cluster is gold.

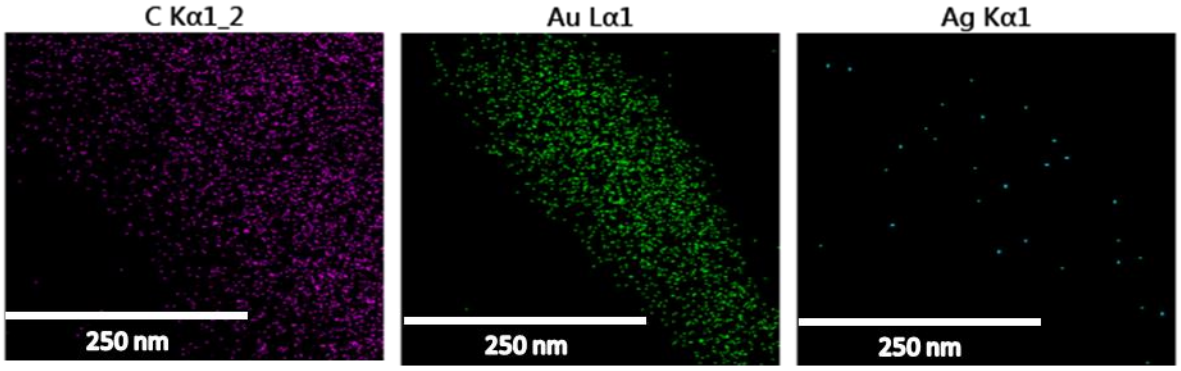

Figure 33: Mapping of the Ag_xAu_{25-x} nanocluster

The figure 34 shows a high resolution TEM image of the sample Ag_xAu_{25-x}, showing particles with different diameter between 4-20 Å indicating the formation of metallic clusters and nanoclusters.

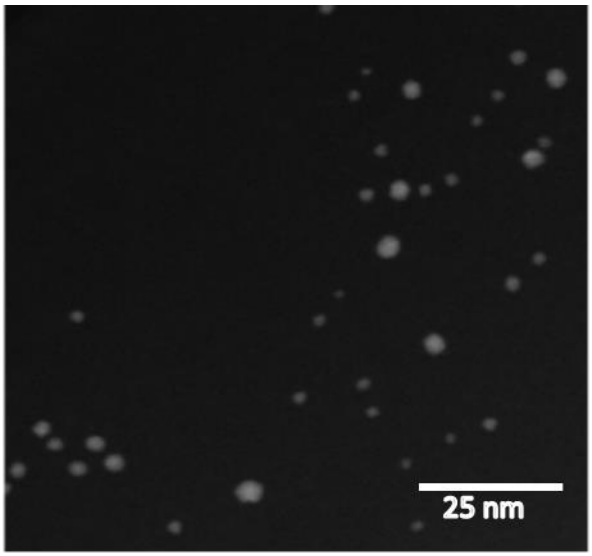

Figure 34: Ag_xAu_{25-x} nanocluster EDS HR-TEM image

The figure 35 shows a high resolution TEM image of one of the zeolites in which the Ag_{25} nanocluster was supported, in the figure is not possible to see any metallic particle on the surface. This does not indicate that there are no silver particles in the sample, but the particles on the surface are very well dispersed and with a very small size. It is well described that supported nanoclusters are not easily observed by electron microscopy.

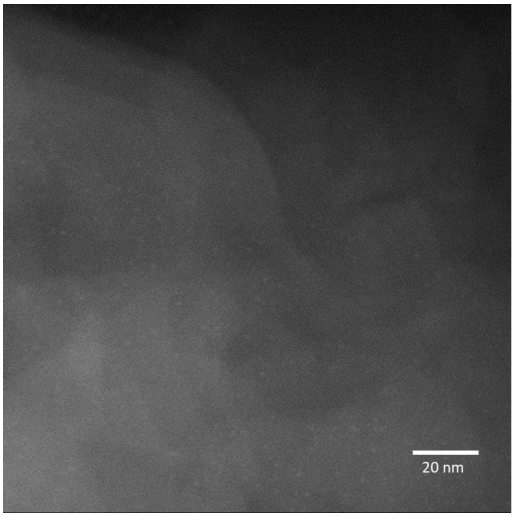

Figure 35: Ag_{25}RTQ511 HR-TEM image

The figure 36 shows the image of the Ag_{25} supported on the pure silica ITQ-2. In this case are observed some bright points that can be related with the silver nanoclusters supported in the zeolite.

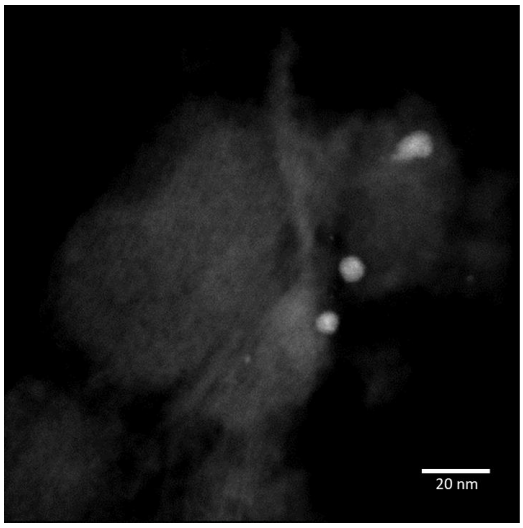

Figure 36: Ag_{25}RTQU46 HR TEM image

In order to check this Energy Dispersive X-ray spectroscopy or EDX was used to detect the presence of silver. In the figure 37 it can be seen an image of the points analyzed by EDX. It was shown that in those points silver appears confirming the formation of Ag nanoclusters.

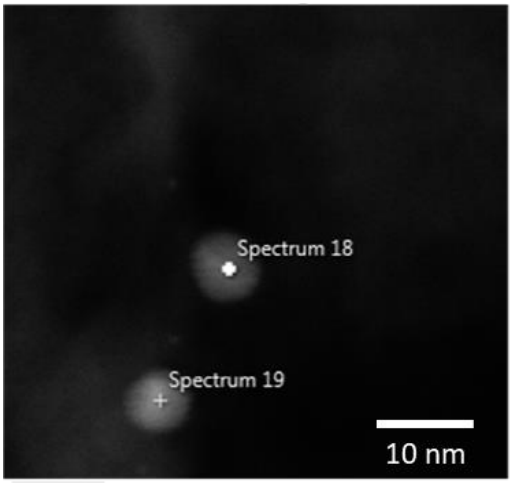

Figure 37: Ag_{25}RTQU46 EDX HR TEM image

The figure 38 and 39 shows TEM pictures of the bimetallic nanocluster supported on the two zeolites RTQ511 and RTQU46. In both images appear bright points that must be related with the metals. Nevertheless, the size is too big for a nanocluster, this does not indicate that Au-Ag nanoclusters are not formed, because this is a punctual technique. But considering that a mixture of fractions was obtained after the synthesis and that nanoparticles are formed in some part of the catalyst; the results indicate that the synthesis method must be improved.

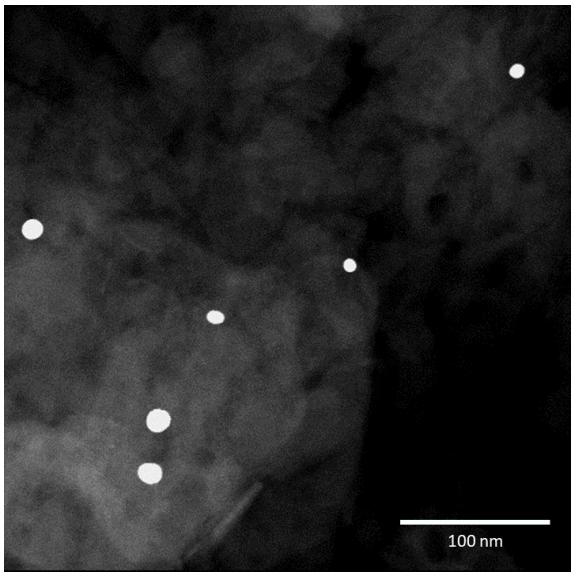

Figure 38: Ag_xAu_{25-x}RTQ511 HR-TEM image

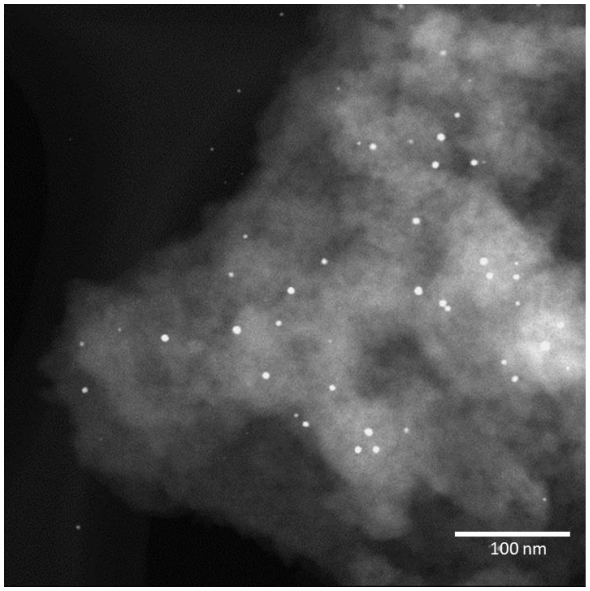

Figure 39: Ag_xAu_{25-x}RTQU46 HR-TEM image

From those results it can be stated that, even the synthesis must be improved, the clusters were synthesized and is supposed that they are well dispersed on the surface of the zeolite but further investigation of the catalysts prepared will be necessary.

4.2 CATALYTIC ACTIVITY

The catalytic tests were conducted with both zeolites containing Ag_{25} and Ag-Au nanoclusters.

The figure 40 shows the catalytic results for the zeolite RTQU46 with nanocluster of silver with 25 atoms activated with air or with H_2 and the results are compared with those of the thermal oxidation (in absence of catalyst)

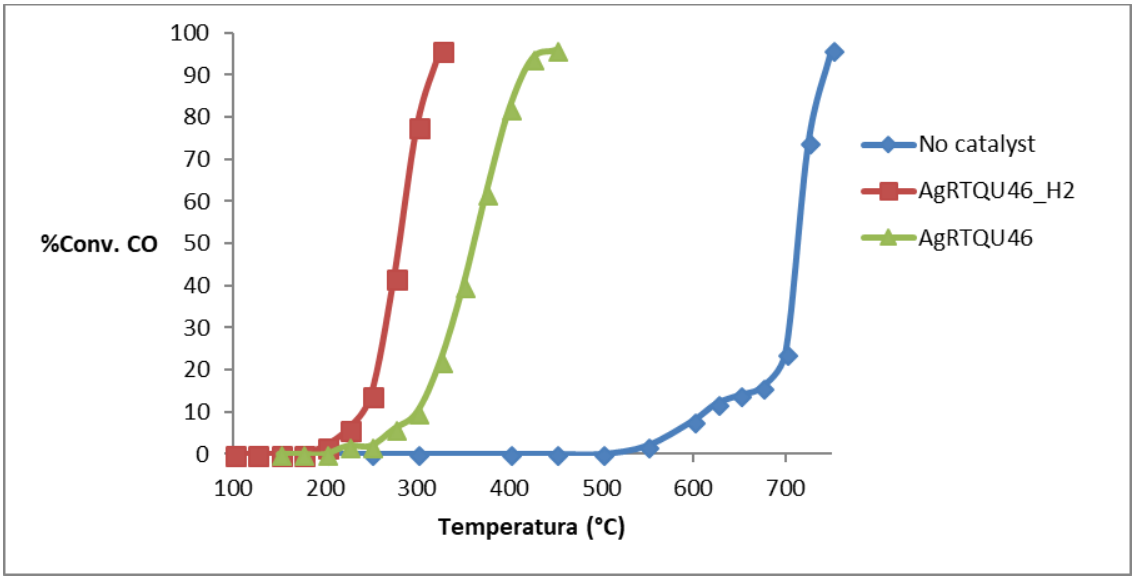

Figure 40: CO oxidation catalyzed by AgRTQU46 with and without hydrogenation (-H_2 means activated with H_2)

As can be seen, the presence of the catalyst substantially reduces the temperature necessary to reach a complete CO conversion. With the catalyst the conversion starts about 200-250°C achieving an almost complete conversion (95%) at 400°C with the catalyst without hydrogenation (AgRTQU46) and at 300°C with the hydrogenated catalyst (AgRTQU46), while the reaction without catalyst reach the maximum conversion at 750°C. These results show that the catalyst prepared are very active and that the activation of the catalyst by hydrogen results in an improvement of the catalyst performance if compares with the catalyst activated with air.

These results were also compared with the results obtained with the zeolite RTQU46 impregnated with the gold-silver clusters (AuAgRTQU46) hydrogenated (purple) and activated with air (orange). This is shown on the figure 41:

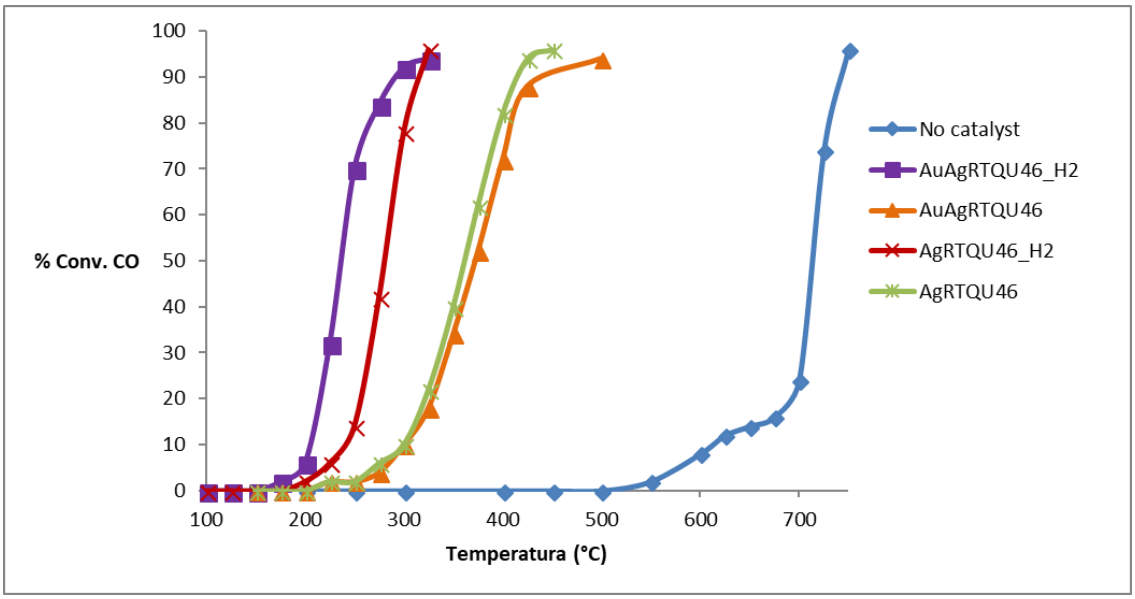

Figure 41: CO oxidation catalyzed by AgRTQU46 and AuAgRTQU46 with and without hydrogenation (-H_2 means activated with H_2).

The bimetal catalysts suppose an improvement, with respect to the catalysts of silver, when the catalyst has been hydrogenated, but similar results were obtained when the samples is activated with air. The difference observed with the samples treated with H_2 could indicate that the reduction with H_2 activate the catalytic sites, being more active the Ag-Au reduced sites than the Ag sites.

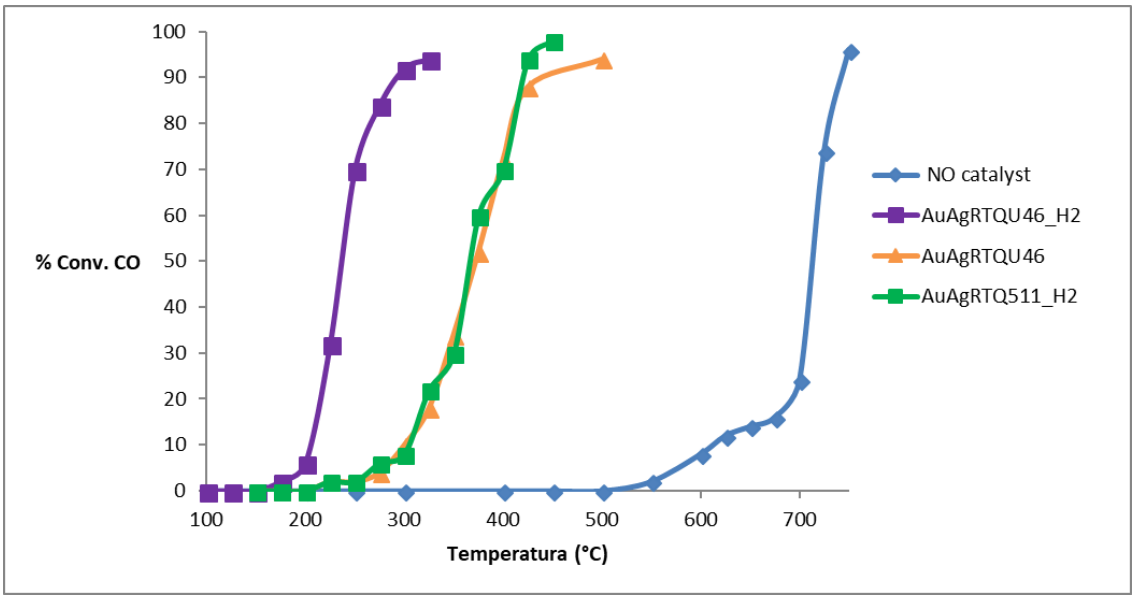

Figure 42: CO oxidation catalyzed by AgRTQU46, AuAgRTQU46 and AuAgRTQ511 (-H_2 means activated with H_2).

The previous results have shown that the best catalyst is that with bimetallic nanocluster activated with H_2, for that reason some nanocluster supported on the other zeolite and activated with H_2 was tested and compared with the previous one.

As it can be seen in the figure 42, the catalyst is active oxidating CO at 300°C. However, the results obtained are necessary worst than those obtained with the catalyst AuAgRTQU46 after hydrogenation. Those results are very similar to those obtained with the zeolites containing nanoclusters but activated with air, indicating that this zeolite prevent the formation of the more active sites formed in the other zeolite after the treatment with H_2.

The RTQU46 zeolite is a pure silica compound without aluminium species in its structure, while the other zeolite the RTQ511 has a Silica/Aluminium relation of 10 (Table 7). The difference in the catalytic activity of both zeolites impregnated with the same cluster suggest that the clusters are better supported and have more catalytical activity on the zeolite without Al, maybe because Al is interacting with the metallic clusters, but more experiments and characterization are necessary to stablish the nature of this interaction.

5. CONCLUSIONS AND OUTLOOK

5.1 CONCLUSIONS

Different thiol-protected silver and bimetallic gold-silver clusters have been synthesized by different methods. In the synthesis of some of them different fractions were obtained and it will be necessary to improve the methods of synthesis in order to get all the clusters pure and ready for the immobilization on oxide materials. A new clusters separation method with PAGE was developed. The materials have been characterized by different techniques. The study by UV-Vis show similar spectra to those reported in bibliography. Nevertheless, is necessary to complement these results with other characterization techniques to know the exact composition of the synthesized clusters because some techniques used in this Master Thesis to characterize them were not successful. The impregnation of the delaminated zeolites with the synthesized clusters was achieved. The results of the catalytic tests performed on the oxidation of carbon monoxide are very promising, showing a high conversion to considerably lower temperatures if compares with the process in the absence of catalyst. It has been shown that the activity of the material depends on the content of Aluminium in the zeolite and in the activation method, obtaining the best results with pure silica zeolites activated with H_2

5.2 OUTLOOK

Further characterization of the crude clusters and the supported clusters need to be performed to gain information about the synthesis reaction and the supporting process. It is necessary to complete the synthesis and supporting on zeolites process with all the clusters synthesized Ag_7, Ag_{32} and perform catalytical test with them. It must also perform new synthesis for the bimetallic clusters with different number of dopant atoms and achieve a precise control of the gold and silver atoms in the samples. This work is expected to be continued by the collaboration between the “Technische Universität Wien” and “Instituto de Tecnologia Química” initiated with this Master Thesis.

6.BIBLIOGRAPHY

1. Yamazoe, S., K. Koyasu, and T. Tsukuda, *Nonscalable Oxidation Catalysis of Gold Clusters.* Accounts of Chemical Research, 2014. **47**(3): p. 816-824.
2. R Kubo, a. A Kawabata, and S. Kobayashi, *Electronic Properties of Small Particles.* Annual Review of Materials Science, 1984. **14**(1): p. 49-66.
3. Negishi, Y., et al., *A Critical Size for Emergence of Nonbulk Electronic and Geometric Structures in Dodecanethiolate-Protected Au Clusters.* Journal of the American Chemical Society, 2015. **137**(3): p. 1206-1212.
4. Brust, M., et al., *Synthesis of thiol-derivatised gold nanoparticles in a two-phase Liquid–Liquid system.* Journal of the Chemical Society, Chemical Communications, 1994(7): p. 801-802.
5. *Frontiers of Nanoscience*, in *Frontiers of Nanoscience*, T. Tsukuda and H. Häkkinen, Editors. 2015, Elsevier. p. ii.
6. Lei, Y., et al., *Increased Silver Activity for Direct Propylene Epoxidation via Subnanometer Size Effects.* Science, 2010. **328**(5975): p. 224-228.
7. Urushizaki, M., et al., *Synthesis and Catalytic Application of Ag44 Clusters Supported on Mesoporous Carbon.* The Journal of Physical Chemistry C, 2015. **119**(49): p. 27483-27488.
8. Briceño, S. and H. Del Castillo, *Reducción catalítica de NOx con Pt soportado sobre zeolitas MFI modificadas con Cu, Co, Fe, Mn.* Avances en Química, 2008. **3**(1).
9. Shimizu, K., K. Sawabe, and A. Satsuma, *Unique catalytic features of Ag nanoclusters for selective NO x reduction and green chemical reactions.* Catalysis Science & Technology, 2011. **1**(3): p. 331-341.
10. Christensen, S.L., et al., *Dopant Location, Local Structure, and Electronic Properties of Au24Pt(SR)18 Nanoclusters.* The Journal of Physical Chemistry C, 2012. **116**(51): p. 26932-26937.
11. Yao, C., et al., *Mono-cadmium vs Mono-mercury Doping of Au25 Nanoclusters.* Journal of the American Chemical Society, 2015. **137**(49): p. 15350-15353.
12. Negishi, Y., et al., *Effect of Copper Doping on Electronic Structure, Geometric Structure, and Stability of Thiolate-Protected Au25 Nanoclusters*. Vol. 3. 2012. 2209–2214.
13. Sels, A., et al., *Structural Investigation of the Ligand Exchange Reaction with Rigid Dithiol on Doped (Pt, Pd) Au25 Clusters.* The Journal of Physical Chemistry C, 2017. **121**(20): p. 10919-10926.
14. Philip, R., et al., *Picosecond optical nonlinearity in monolayer-protected gold, silver, and gold-silver alloy nanoclusters.* Physical Review B, 2000. **62**(19): p. 13160-13166.
15. Salazar, M., R. Becker, and W. Grünert, *Hybrid catalysts—an innovative route to improve catalyst performance in the selective catalytic reduction of NO by NH3.* Applied Catalysis B: Environmental, 2015. **165**: p. 316-327.
16. Cheng, J., R. Xu, and G. Yang, *Synthesis, structure and characterization of a novel germanium dioxide with occluded tetramethylammonium hydroxide.* Journal of the Chemical Society, Dalton Transactions, 1991(6): p. 1537-1540.
17. Maia, G.D.N., et al., *Ammonia biofiltration and nitrous oxide generation during the start-up of gas-phase compost biofilters.* Atmospheric Environment, 2012. **46**: p. 659-664.
18. Corma, A., et al., *Delaminated zeolite precursors as selective acidic catalysts.* Nature, 1998. **396**: p. 353.
19. Opanasenko, M.V., W.J. Roth, and J. Čejka, *Two-dimensional zeolites in catalysis: current status and perspectives.* Catalysis Science & Technology, 2016. **6**(8): p. 2467-2484.

20. Krishnadas, K.R., et al., *Structure-conserving spontaneous transformations between nanoparticles.* Nature Communications, 2016. **7**: p. 13447.
21. Udayabhaskararao, T., M.S. Bootharaju, and T. Pradeep, *Thiolate-protected Ag32 clusters: mass spectral studies of composition and insights into the Ag-thiolate structure from NMR.* Nanoscale, 2013. **5**(19): p. 9404-9411.
22. Kumar, S., M.D. Bolan, and T.P. Bigioni, *Glutathione-Stabilized Magic-Number Silver Cluster Compounds.* Journal of the American Chemical Society, 2010. **132**(38): p. 13141-13143.
23. Bootharaju, M.S. and T. Pradeep, *Facile and Rapid Synthesis of a Dithiol-Protected Ag7 Quantum Cluster for Selective Adsorption of Cationic Dyes.* Langmuir, 2013. **29**(25): p. 8125-8132.
24. Wu, Z., et al., *High Yield, Large Scale Synthesis of Thiolate-Protected Ag7 Clusters.* Journal of the American Chemical Society, 2009. **131**(46): p. 16672-16674.
25. Joshi, C.P., et al., *[Ag25(SR)18]−: The "Golden" Silver Nanoparticle.* Journal of the American Chemical Society, 2015. **137**(36): p. 11578-11581.
26. Negishi, Y., T. Iwai, and M. Ide, *Continuous modulation of electronic structure of stable thiolate-protected Au25 cluster by Ag doping.* Chemical Communications, 2010. **46**(26): p. 4713-4715.
27. Negishi, Y., et al., *Isolation, structure, and stability of a dodecanethiolate-protected Pd1Au24 cluster.* Physical Chemistry Chemical Physics, 2010. **12**(23): p. 6219-6225.
28. Negishi, Y., et al., *Origin of Magic Stability of Thiolated Gold Clusters: A Case Study on Au25(SC6H13)18.* Journal of the American Chemical Society, 2007. **129**(37): p. 11322-11323.
29. Mori, S. and H.G. Barth, *Size Exclusion Chromatography*. 2013: Springer Berlin Heidelberg.
30. Walsh, E.J., *Biochemistry (Garrett, Reginald H.; Grisham, Charles M.).* Journal of Chemical Education, 1997. **74**(2): p. 189.
31. Davis, L., *Basic Methods in Molecular Biology*. 2012: Elsevier Science.
32. Baekelant, W., et al., *Form Follows Function: Warming White LEDs Using Metal Cluster-Loaded Zeolites as Phosphors.* ACS Energy Letters, 2017. **2**(10): p. 2491-2497.
33. Fujiwara, K., et al., *Synthesis of Ag nanoparticles encapsulated in hollow silica spheres for efficient and selective removal of low-concentrated sulfur compounds.* Journal of Materials Chemistry A, 2017. **5**(48): p. 25431-25437.
34. Horta-Fraijo, P., et al., *Ultra-small Ag clusters in zeolite A4: Antibacterial and thermochromic applications.* Physica E: Low-dimensional Systems and Nanostructures, 2018. **97**: p. 111-119.
35. Yu, Y., et al., *Scalable and Precise Synthesis of Thiolated Au10–12, Au15, Au18, and Au25 Nanoclusters via pH Controlled CO Reduction.* Chemistry of Materials, 2013. **25**(6): p. 946-952.
36. Yang, H., et al., *All-thiol-stabilized Ag44 and Au12Ag32 nanoparticles with single-crystal structures.* Nature Communications, 2013. **4**: p. 2422.
37. Tlahuice-Flores, A., *Ligand effects on the structure and vibrational properties of the thiolated Au18 cluster.* Progress in Natural Science: Materials International, 2016. **26**(5): p. 510-515.
38. Tlahuice-Flores, A., R.L. Whetten, and M. Jose-Yacaman, *Vibrational Normal Modes of Small Thiolate-Protected Gold Clusters.* The Journal of Physical Chemistry C, 2013. **117**(23): p. 12191-12198.
39. Varnholt, B., et al., *Structural Information on the Au–S Interface of Thiolate-Protected Gold Clusters: A Raman Spectroscopy Study.* The Journal of Physical Chemistry C, 2014. **118**(18): p. 9604-9611.
40. Yao, Q., et al., *Precise control of alloying sites of bimetallic nanoclusters via surface motif exchange reaction.* Nature Communications, 2017. **8**(1): p. 1555.

41. Desireddy, A., et al., *Ultrastable silver nanoparticles.* Nature, 2013. **501**: p. 399.
42. Guo, J., et al., *Mass Spectrometric Identification of Silver Nanoparticles: The Case of Ag32(SG)19.* Analytical Chemistry, 2012. **84**(12): p. 5304-5308.